

# Presupernova evolution and explosion of massive stars with mass loss

M. Limongi<sup>\*,†</sup> and A. Chieffi<sup>\*\*‡</sup>

<sup>\*</sup>*INAF - Osservatorio Astronomico di Roma, Via Frascati 33, I-00040, Rome, Italy*

<sup>†</sup>*Department of Astronomy, University of Tokyo, Bunkyo-ku, Tokyo 113-0033, Japan*

<sup>\*\*</sup>*INAF - Istituto di Astrofisica Spaziale e Fisica Cosmica, Via Fosso del Cavaliere, I-00133, Rome, Italy*

<sup>‡</sup>*Centre for Stellar and Planetary Astrophysics, School of Mathematical Sciences, P.O. Box 28M, Monash University, Victoria 3800, Australia*

## Abstract.

We review the main properties of solar metallicity massive stars in the range 11-120  $M_{\odot}$ . The influence of the mass loss on the hydrostatic burning stages as well as the final explosion is discussed in some detail. We find that the minimum masses that enter the WNL, WNE and WC stages are 30  $M_{\odot}$ , 35  $M_{\odot}$  and 40  $M_{\odot}$  respectively; the limiting mass between stars exploding as SNII and SN Ib/c is between 30 and 35  $M_{\odot}$ ; the limiting mass between stars forming neutron stars and black holes after the explosion is between 25-30  $M_{\odot}$ . We also discuss the properties of the chemical yields integrated over a Salpeter IMF and we find that stars with  $M \geq 35 M_{\odot}$  contribute for  $\sim 60\%$  to the production of C, N and for  $\sim 40\%$  to the production Sc and s-process elements up to Zr, while they do not produce any intermediate mass element because of the large remnant masses.

**Keywords:** Stellar Evolution, Nucleosynthesis, Supernovae

**PACS:** 97.10.Cv, 97.10.Me, 97.60.-s, 97.60.Bw, 26.20.+f, 26.30.+k

## INTRODUCTION

Massive stars, i.e. the stars that evolve through all the hydrostatic nuclear burning stages in a quiescent way up to the explosion, play a key role in many astrophysical fields. They light up regions of stellar birth, may induce star formation, produce most of the elements, especially those necessary to life, are responsible for the mixing of the interstellar medium and also contribute to the production of neutron stars and black holes. For all these reasons they play a pivotal role in the evolution of the galaxies. Massive stars also produce some long-lived radioactive isotopes like, e.g.,  $^{26}\text{Al}$ ,  $^{44}\text{Ti}$ ,  $^{56}\text{Co}$ ,  $^{60}\text{Fe}$ , whose radioactive transitions may give rise to  $\gamma$ -ray photons that can be detected by sufficiently sensitive instruments presently in space (INTEGRAL, RHESSI). The measurements of the  $\gamma$ -ray signals from the decay of species with lifetimes shorter than those typical of the evolution of the Galaxy clearly demonstrate that nucleosynthesis is still active today. Last, but not least, the collapse of massive stars is likely responsible to the processes leading to some kind of Gamma Ray Burst events. Massive stars are of such astrophysical relevance that a proper understanding of their evolution and explosion is mandatory.

In this review we will briefly discuss the main evolutionary properties of almost the full range of massive stars (i.e. between 11 and 120  $M_{\odot}$ ) of initial solar composition during all the hydrostatic burning stages from the main sequence phase up to the onset of

the iron core collapse. Special attention will be paid to the effects of mass loss. We will also discuss the basic properties of their explosive yields together to their contribution to the chemical evolution of the Galaxy.

## THE STELLAR MODELS

All the models presented in this paper have been computed by means of the latest version of the FRANEC that is described in detail in [1]. Let us just mention here that mass loss is included following [2] for the blue supergiant phase, and [3] for the red supergiant phase. For the Wolf-Rayet phase the mass loss rate provided by [4] has been adopted. The models have initial solar composition [5] and range in mass between 11 and 120  $M_{\odot}$ .

## H AND HE BURNING

The core H burning is the first nuclear burning stage and, in these stars, is powered by the CNO cycle. The strong dependence of this cycle on the temperature implies the presence of a convective core that reaches its maximum extension just at the beginning of the central H burning and that then recedes in mass as the central H is burnt. Mass loss is quite efficient during this phase and increases substantially with the luminosity of the star (i.e. the initial mass). It leads to a significant reduction of the total mass of the star in stars initially more massive than  $\sim 40 M_{\odot}$ . For example, the 60  $M_{\odot}$  model has a total mass at core H exhaustion equal to 38  $M_{\odot}$  while the 120  $M_{\odot}$  ends the H burning as a 56  $M_{\odot}$ . The mass loss rate in this phase typically ranges from  $10^{-6} M_{\odot}/\text{yr}$  for the 40  $M_{\odot}$  to  $10^{-5} M_{\odot}/\text{yr}$  for the 120  $M_{\odot}$ . Most of the massive stars spend a significant fraction of their central H burning lifetime as O-type stars (i.e. have effective temperatures ranging between 50000 K  $< T_{\text{eff}} < 33000$  K) and the minimum mass that becomes an O-type star is the 14  $M_{\odot}$  in our set of models (Figure 1). The fraction of H burning lifetime spent by a star as an O-type star increases with the initial mass and varies from  $\sim 15\%$  for the 14  $M_{\odot}$  to  $\sim 80\%$  for the 120  $M_{\odot}$ . The H exhausted core (He core) that forms at the central H exhaustion scales (in mass size) directly with the initial mass. It is worth noting here that the presently adopted mass loss rates in the blue supergiant phase do not alter too much the initial mass-He core mass at the core H exhaustion. For example, the He core mass of a 80  $M_{\odot}$  model at core H exhaustion without mass loss is 26  $M_{\odot}$  while for the same model with mass loss it reduces to 22  $M_{\odot}$ , i.e., only by  $\sim 5\%$ , although the total mass is reduced to 47  $M_{\odot}$ , i.e., by  $\sim 40\%$ . On the contrary the size of the H convective core, which in turn may be affected by the overshooting and/or semiconvection, has a strong impact on the initial mass-He core mass relation and hence constitutes the greatest uncertainty in the computation of the core H burning phase.

At the core H exhaustion all the models move toward the red side of the HR diagram while the centre contracts until the core He burning begins. The further fate of the models is largely driven by the competition between the efficiency of mass loss in reducing the H rich envelope during the RSG phase and the core He burning timescale. Note that, as soon as the star expands and cools, the mass loss rate switches from that provided by [2]

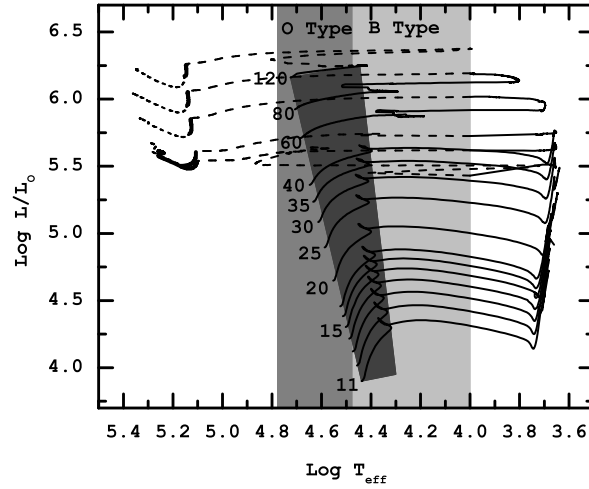


**FIGURE 1.** Evolutionary paths of the stellar models in the HR diagram. The *dark – grey* shaded area marks the location of core H burning models. The *dashed, thick – solid* and *dotted* lines refer to the WNL, WNE and WC stages respectively. Also shown are the regions corresponding to the O-type and B-type stars.

to that given by [3]. Stars initially less massive than  $30 M_{\odot}$  do not lose most of their H rich mantle hence they will live up to the onset of the core collapse and explode as red supergiants. Vice versa stars initially more massive than this threshold value lose enough mass to end their life as WR stars. However, also these stars may spend a fraction of their He burning lifetime as red supergiants before becoming WR stars. The fraction of core He burning lifetime spent by one of these stars as a RSG ( $\tau_{\text{red}}/\tau_{\text{He}}$ ) obviously depends on the efficiency of the mass loss and since it increases significantly with the luminosity (that in turn depends on the initial mass of the star), the larger the mass the higher the mass loss rate and the smaller the percentage of time spent by a star as a red supergiant. For example the  $35 M_{\odot}$  becomes a WNL star when the central He mass fraction is 0.52 and  $\tau_{\text{red}}/\tau_{\text{He}} \sim 0.38$ , while in the  $80 M_{\odot}$  the transition from RSG to BSG occurs when the central He mass fraction is 0.95 and hence  $\tau_{\text{red}}/\tau_{\text{He}}$  is less than 0.002. The  $120 M_{\odot}$  never moves to the red because it becomes a WNL already during the latest stages of core H burning. It is worth noting here that when a star becomes a Wolf-Rayet the mass loss rate typically reduces by about one order of magnitude compared to that in the RSG phase [4]. When the surface H mass fraction abundance drops below roughly 0.4 the star quickly moves to the blue side of the HR diagram and continues the core He burning as a WR star. As it is well known, central He burning occurs in a convective core whose mass size either advances in mass or remains fixed (at most). Such a behavior, typical in stars in which the He core mass does not shrink in mass during the central He burning, changes in the models in which the He core mass reduces during the central He burning (i.e. the WNE/WC/WO stars). The stars that in our set of models become at least WNE WR stars (i.e., the ones having  $X_{\text{sup}} < 10^{-5}$  and  $(C/N)_{\text{sup}} < 0.1$  according to the standard definition) are those with  $M \geq 35 M_{\odot}$ . Once the full H rich mantle is lost, the further evolution of the stellar model depends on the actual He core mass. In fact, as the He core is reduced by mass loss the star feels this reduction and tends to

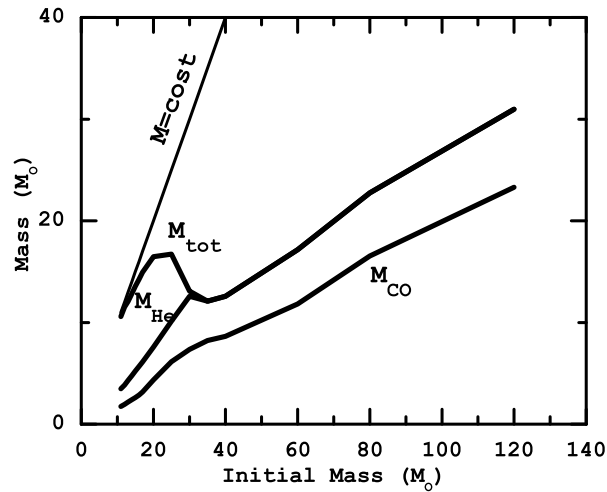


**FIGURE 2.** Total mass, He core mass and CO core mass as a function of the initial mass at core He exhaustion.

behave like a star of a smaller mass (i.e., a star having the same actual He core mass). Hence, the reduction of the He core (i.e. the total mass) during the core He burning has the following effects: 1) the He convective core reduces progressively in mass, 2) the He burning lifetime increases, 3) the luminosity progressively decreases, 4) the  $^{12}\text{C}$  mass fraction at core He exhaustion is higher than it would be without mass loss and 4) the CO core at the core He exhaustion resemble that of other stars having similar He core masses independently on the initial mass of the star.

Stars with mass  $M \geq 40 M_{\odot}$  (in our scenario) experience a mass loss strong enough that the total mass is decreased down to the mass coordinate marking the maximum extension of the He convective core. Once this happens, the star becomes a WC Wolf-Rayet star (i.e., when  $(\text{C}/\text{N})_{\text{sup}} > 10$  according to the standard definition) and the products of core He burning are exposed to the surface and ejected into the interstellar medium through their stellar wind.

Figure 2 shows the He and the CO core masses at core He exhaustion as a function of the initial mass. It is worth noting that, independently on the total amount of mass lost, the CO core shows a clear one to one trend with the mass in the whole range of masses. Before closing this section it is worth reminding that obviously the mass loss during both the RSG and the WR phases has a strong impact on the WR lifetime and on the specific lifetimes in the various WR stages. Let us recall here few basic rules: 1) the higher the mass loss during the RSG phase the earlier the stage (the higher the central He mass fraction) at which the star enters the WR phase; 2) the higher the amount of mass lost during the WR phase the lower the actual size of the He core, the longer the He burning lifetimes and hence the longer the WR lifetime.

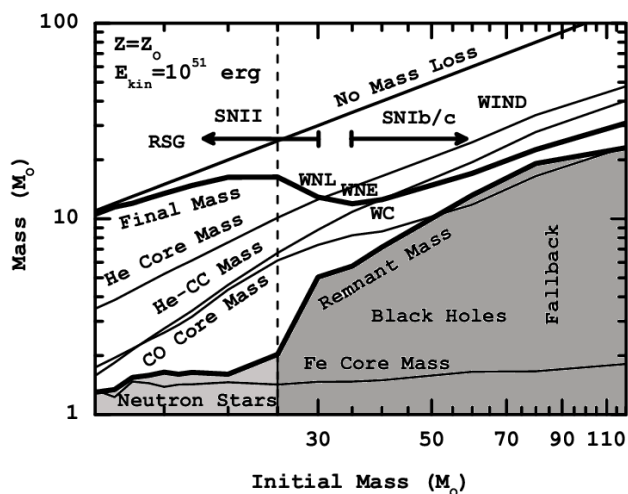


**FIGURE 3.** Final masses and remnant masses (*thick – solid lines*) as a function of the initial mass by assuming that all the models have  $E_{\text{kin}} = 10^{51}$  erg. Also shown are the maximum He core, He convective core and CO core masses, the minimum masses that enter the various stages of WR, the limiting mass between stars exploding as SNII and SNIb/c, the limiting mass between stars forming neutron stars and black holes after the explosion.

## THE ADVANCED BURNING STAGES

The nuclear burning stages that follow the central He exhaustion up to the presupernova stage have been extensively discussed in the literature [6, 7, 8, 9, 10] and hence here we just recall few basic properties. The advanced burning evolutionary stages are characterized by a strong neutrino emission, the neutrinos being mainly produced by pairs production in the center of the star. From the central C burning onward, the neutrino luminosity progressively increases and supersedes the photon luminosity [7] by several orders of magnitude (up to  $\sim 8$ ) and hence the advanced nuclear burnings must speed up enormously in order to counterbalance such dramatic energy losses. This also means that the region outside the CO core mass remains essentially frozen out during the advanced burning phases up to the moment of the explosion.

The evolution of the star during the advanced burning stages is mainly driven by the size and the composition ( $^{12}\text{C}/^{16}\text{O}$ ) of the CO core. In general each burning stage, from the C burning up to the Si burning, occurs first at the center and then, as the fuel is completely burnt, it shifts in a shell. The nuclear burning shell, then, may induce the formation of one or more successive convective zones, that can partially overlap. The general trend is that the number of convective shells scales inversely with the mass size of the CO core. For example in the  $11 M_{\odot}$  model, four consecutive C convective shells form while in the  $60 M_{\odot}$  model only one. The complex interplay among burning shells and convective zones determines, in a direct way, not only the chemical composition but also the final mass-radius relation inside the CO core at the presupernova stage. In general, the more efficient the shell burning is, the smaller the number of convective shells, the slower is the contraction and the shallower is the final mass-radius relation, i.e., the higher is the mass of the star the more compact is the CO core.

## SIMULATED EXPLOSION AND EXPLOSIVE NUCLEOSYNTHESIS

The chemical composition left by the hydrostatic evolution is partially modified by the explosion, especially that of the more internal zones. At present there is no self consistent hydrodynamical model for core collapse supernovae and consequently we are forced to simulate the explosion in some way in order to compute the explosive yields. The idea is to deposit a given amount of energy at the base of the exploding envelope and follow the propagation of the shock wave that forms by means of a hydro code. The initial amount of energy is fixed by requiring a given amount of kinetic energy at the infinity (typically of the order of  $10^{51}$  erg = 1 foe). Whichever is the technique adopted to deposit the energy into the presupernova model (piston, kinetic bomb or thermal bomb), in general the result is that some amount of material (the innermost one) will fall back onto the compact remnant while most of the envelope will be ejected with the desired final kinetic energy. The mass separation between remnant and ejecta is always referred to as the mass cut. The propagation of the shock wave into the exploding envelope induces compression and local heating and hence explosive nucleosynthesis. Zones heated up to different peak temperatures undergo different kind of explosive nucleosynthesis: complete explosive Si burning (for  $T_{\text{peak}} > 5 \cdot 10^9$  K), incomplete explosive Si burning (for  $4 \cdot 10^9$  K  $< T_{\text{peak}} < 5 \cdot 10^9$  K), explosive O burning (for  $3.3 \cdot 10^9$  K  $< T_{\text{peak}} < 4 \cdot 10^9$  K), explosive Ne burning (for  $2.1 \cdot 10^9$  K  $< T_{\text{peak}} < 3.3 \cdot 10^9$  K) and explosive C burning (for  $1.9 \cdot 10^9$  K  $< T_{\text{peak}} < 2.1 \cdot 10^9$  K). Matter heated up to temperatures lower than, say,  $T_{\text{peak}} = 1.9 \cdot 10^9$  K is not affected by the explosion due to the very short explosion timescales. Since the matter behind the shock is radiation dominated, the peak temperature at which each zone is heated up during the explosion is given by  $T_{\text{peak}} = (3E/(4\pi a R_{\text{PN}}^3))^{1/4}$ , where  $R_{\text{PN}}$  is the presupernova radius. By means of this equation, at each explosive burning corresponds a given volume of the star. As a consequence, the mass-radius relation at the presupernova stage determines the amount of mass exposed to each explosive burning. Following this rule, the more massive stars (i.e., those more compact) will produce much more heavy elements (i.e., those produced by the explosive burnings) than the less massive ones. However, the steeper is the mass-radius relation the higher is the binding energy and hence the larger will be, in general, the mass falling back onto the compact remnant. Figure 3 shows the initial mass-final mass relation in the assumption that the ejecta have 1 foe of kinetic energy at the infinity in all the models - the explosions have been carried out in the framework of the kinetic bomb. This choice (i.e.,  $E_{\text{kin}} = 1$  foe for all the models) implies that in stars with masses above 25-30  $M_{\odot}$  all the CO core, or a great fraction of it, fall back onto the compact remnant. As a consequence these stars would not eject any product of the explosive burnings as well as those of the C convective shell and will leave, after the explosion, black holes with masses ranging between 3 and 11  $M_{\odot}$ . In figure 3 there are also shown the limiting masses that enter the various WR stages, i.e., WNL (30  $M_{\odot}$ ), WNE (35  $M_{\odot}$ ) and WC (40  $M_{\odot}$ ), as well as the limiting mass (30- 35  $M_{\odot}$ ) between stars exploding as Type II SNe and those exploding as Type Ib/c supernovae. These results, however, must be taken with caution because they depends on many uncertainties related to the both the hydrostatic evolution (mainly mass loss) and the explosion (mainly the final kinetic

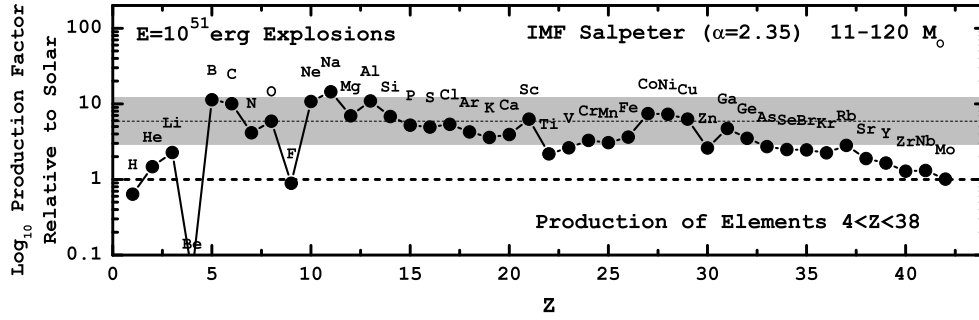


**FIGURE 4.** Production factors of a generation of massive stars in the range 11-120  $M_{\odot}$  integrated over a Salpeter IMF. All the models have  $E_{\text{kin}} = 1$  foe at infinity.

energy at the infinity). How this picture changes by changing the mass loss and the final kinetic energy will be discussed in a forthcoming paper.

## INTEGRATED CHEMICAL YIELDS

The first products of the calculations described above are the yields of the various isotopes, i.e., the amount of mass of each isotope ejected by each star in the interstellar medium. The integration of these yields over an initial mass function (IMF) provide the chemical composition of the ejecta of a generation of massive stars. Figure 4 shows the production factors of all the elements obtained by assuming a Salpeter IMF ( $dn/dm = km^{-2.35}$ ) provided by a generation of massive stars in the range 11-120  $M_{\odot}$ . This figure clearly shows that these stars are responsible for producing all the elements with  $4 < Z < 38$ . Moreover, the majority of the elements preserve a scaled solar distribution relative to O. Other sources, like, e.g. AGB stars and Type Ia SNe, must contribute to all the elements that are under produced by massive stars (e.g., the iron peak elements and the s-process elements above Ge). The contribution of the more massive stars, e.g., stars with  $M \geq 35 M_{\odot}$ , to the total yield of each element is shown in Figure 5. These more massive stars produce roughly  $\sim 60\%$  of the total yields of C and N and about  $\sim 40\%$  of Sc and s-process elements. This is the result of the strong mass loss experienced by these stars that allows the ejection of these elements, synthesized during H (N) and He burning (C, Sc and s-process elements), before their destruction during the more advanced burning stages and/or during the explosion. On the contrary, these stars do not contribute at all to the production of all the intermediate mass and iron peak elements because of their large remnant masses.

## SUMMARY AND CONCLUSIONS

In this paper we briefly reviewed the main evolutionary properties of massive stars during both hydrostatic and explosive stages. The role of mass loss has been discussed in some detail. We found the following results: 1) stars with  $M \leq 25 M_{\odot}$  explode as RSG while stars above this limit explode as BSG; 2) the minimum masses the enter the WNL,

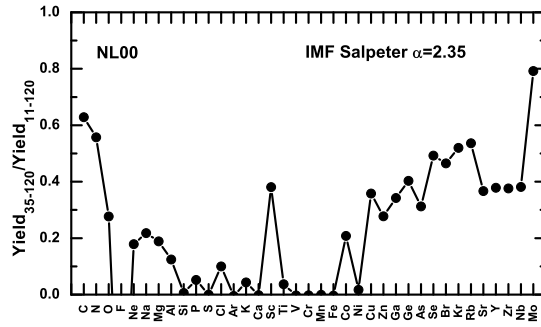


**FIGURE 5.** Contribution of stars with  $M \geq 35 M_{\odot}$  to the total yields of a generation of massive stars in the range 11-120  $M_{\odot}$  integrated over a Salpeter IMF. All the models have  $E_{\text{kin}} = 1$  foe at infinity.

WNE and WC stages are 30  $M_{\odot}$ , 35  $M_{\odot}$  and 40  $M_{\odot}$  respectively; 3) the limiting mass between stars exploding as SNI and SNIb/c is between 30 and 35  $M_{\odot}$  and implies a SNIb/c/SNI ratio of 0.22 when a Salpeter IMF is adopted; 4) the limiting mass between stars forming neutron stars and black holes after the explosion is between 25-30  $M_{\odot}$ ; 5) assuming a Salpeter IMF, stars with  $M \geq 35 M_{\odot}$  contribute for  $\sim 60\%$  to the production of C and N, and for  $\sim 40\%$  to the production Sc and s- process elements up to Zr, while they do not produce any intermediate mass element because of the large remnant masses.

As a final comment we want to remark that these results are extremely sensitive to many uncertainties among which we emphasize the mass loss and the explosion energy at the infinity. A closer investigation on how these uncertainties affect the picture presented here will be addressed in a forthcoming paper.

## ACKNOWLEDGMENTS

I (ML) would like to thank Ken'ichi Nomoto for many stimulating and helpful discussions and for his very kind and generous hospitality at The University of Tokyo during my visit. This work has been supported in part by 21st Century COE Program (QUEST) from the MEXT of Japan and in part by the Italian Ministry of the Education, University and Research (MIUR) through the grant PRIN- 2004 (Prot. 2004029938).

## REFERENCES

1. M. Limongi, and A. Chieffi, *ApJ*, **647**, 483 (2006)
2. J.S. Vink, A. de Koter and H.J.G.L.M. Lamers, *AA*, **362**, 295 (2000)
3. C. de Jager, H. Nieuwenhuijzen and K.A. van der Hucht, *AAS*, **72**, 259 (1989)
4. T. Nugis, and H.J.G.L.M. Lamers, *AA*, **360**, 227 (2000)
5. E. Anders, and N. Grevesse, *Geochim. Cosmochim. Acta*, **53**, 197 (1989)
6. S.E. Woosley, and T.A. Weaver, *ApJS*, **101**, 181 (1995)
7. M. Limongi, O. Straniero, and A. Chieffi, *ApJS*, **129**, 625 (2000)
8. H. Umeda, and K. Nomoto, *ApJ*, **565**, 385 (2002)
9. M. Limongi, and A. Chieffi, *ApJ*, **592**, 404 (2003)
10. A. Chieffi, and M. Limongi, *ApJ*, **608**, 405 (2004)